Research Article

Emmanuel Mkumbuzi, Bishop Bruce Sithole, and Werner Ewald van Zyl*

Microwave-assisted extraction of acetosolv lignin from sugarcane bagasse and electrospinning of lignin/PEO nanofibres for carbon fibre production

https://doi.org/10.1515/gps-2023-0258
received December 18, 2023; accepted May 22, 2024

Abstract: Sugarcane bagasse (SB) is an agricultural waste with massive potential as a source of lignin for the production of renewable materials. In this study, acetosolv lignin from SB was extracted efficiently and sustainably via microwave (MW)-assisted extraction within 10 min. Subsequently, acetosolv lignin was subjected to electrospinning into lignin nanofibres (LNFs) for carbon fibre production using an 85/15% w/w lignin/poly(ethylene oxide) blend ratio in a DMF solution after optimisation of suitable electrospinning parameters. The structural characterisation of lignin was accomplished via pyrolysis-gas chromatography with mass spectrometry, heteronuclear single quantum coherence, Fourier-transform infrared spectroscopy, size-exclusion chromatography, and thermogravimetric analysis while the electrospun LNFs were characterised by transmission electron microscope as randomly arranged fibres with diameters ~15 nm. SB is a readily available and valuable source of lignin for facile MW extraction using acetic acid, while electrospinning was a fast and efficient method for the fabrication of LNFs.

Keywords: microwave-assisted, delignification, electrospinning, lignin nanofibres, sugarcane bagasse

1 Introduction

Carbon fibres (CF) are highly versatile materials widely used in several sectors of the economy, including aerospace, construction, automotive, and energy [1]. However, at least 50% of the cost of CF production is due to the expensive petroleum-derived polyacrylonitrile (PAN) precursor. Cheaper and renewable PAN alternatives are required to enable the cheaper production of CFs [2,3]. In particular, sustainable lignin carbon fibre (LCF) production using lignin derived from agricultural lignocellulosic wastes such as corn stover, wheat husks, corn cobs, and sugarcane bagasse (SB) are advantageous since they do not compete with food security [4–6]. SB from sugar processing is a good biomass precursor for LCF production; as a material, it has a reasonably steady supply (annual global production is about 500 million tonnes) [5,7], has a centralised source, can easily be collected and transported relatively cheaply, and it has a generally homogenous material composition [8,9].

Although biomass-derived LCFs have been successfully fabricated [10], they tend to be unsuitable for structural applications due to their numerous defects [11]. The voids resulting from the volatilisation of side chains in lignin, carbohydrate impurities, and plasticisers used in lignin blends during the carbonisation process [12]. Nevertheless, LCFs have found important applications in energy storage devices, including supercapacitors [13–15], sodium-ion batteries [15,16], and lithium-ion batteries [17–19], where their voids are beneficial as they enable a greater intercalation volume for ions used in energy storage [20,21]. LCFs have also been successfully used as adsorbents for water purification and remediation [22,23] and as catalyst support in heterogeneous catalysis [24,25].

The most common techniques used in the fractionation/extraction of the lignin, the LCF precursor, from biomass, such as the Kraft, soda, and sulphite processes, generally use environmentally harmful chemicals while also being energy-intensive and time-consuming [26,27]. In addition, impure lignin by-product contaminated by inorganic contaminants, with limited application downstream, is often produced, relegating copious amounts of lignin by-product to underutilisation as boiler fuel in the biorefinery [21,28–31]. Efficient and environmentally benign lignin extraction processes producing lignin with fewer inorganic contaminants are critical for lignin valorisation [4,32–34]. In this regard, organic solvents

* **Corresponding author: Werner Ewald van Zyl**, School of Chemistry and Physics, University of KwaZulu-Natal, Westville Campus, Durban, 4000, South Africa, e-mail: vanzylw@ukzn.ac.za, tel: +27 (0)31 260 3188
Emmanuel Mkumbuzi: School of Chemistry and Physics, University of KwaZulu-Natal, Westville Campus, Durban, 4000, South Africa
Bishop Bruce Sithole: Council for Scientific and Industrial Research (CSIR), University of KwaZulu-Natal, Durban, 4125, South Africa

such as formic acid, acetic acid (AA), methanol, and ethanol have been touted as crucial solvents in lignin extraction [35]; in addition, these solvents can be produced on-site by the biorefineries from the holocellulose components (hemicellulose and cellulose) of the same biomass, encouraging a circular bio-economy overall [35–40].

By following sound circular economy principles, including biomass fractionation and subsequent LCF production, several techniques have been developed. To enable efficient lignin extraction, organic solvents have been coupled with external non-ionising radiation such as microwaves (MW), dramatically reducing extraction time and efficiently extracting the lignin [41,42]. MW-assisted heating has higher heating rates compared to conventional heating, whose vessels are slower to warm up. In MW-assisted heating, the energy is transferred more efficiently to the material electromagnetically, rather than via a thermal heat flux down a thermal gradient, as with traditional heating methods [43–49].

The efficiency of MW irradiation derives from the rapid volumetric heating [43–49], which is generated by the swift migration of ions and rotation of dipoles in molecules, resulting in molecular friction and heat generation. Successful MW lignin extractions from biomass using organic solvents have been achieved using bamboo in a formic acid/AA/water solution with 6% HCl [50], birch in formic acid [31], and SB in 90% (v/v) AA and 2% HCl [42].

After extracting the lignin precursor, efficient and economical lignin nanofibre (LNF) production is also vital, and can be achieved using electrospinning [21,51,52]. Electrospinning is a well-established technique that uses electrostatic forces to fabricate non-woven fibre mats with typically randomly oriented fibres spanning the submicron to micron range in diameter [19,53,54].

Electrospinning is achieved by applying a high voltage to a fluid polymer, inducing an electric charge in the fluid. Once a critical charge is reached, a fluid jet will be formed from the droplet at the needle's tip and travel towards the region of lower potential (grounded collector) where the fibres will be collected [55]. The electrospinning setup can be horizontally or vertically oriented, or even be a rotating drum to allow for the formation of aligned fibres (Figure 1) [56–58]. The overall fibre morphology produced via electrospinning depends on several variables, such as the lignin type, solvent, binder polymer, viscosity of lignin

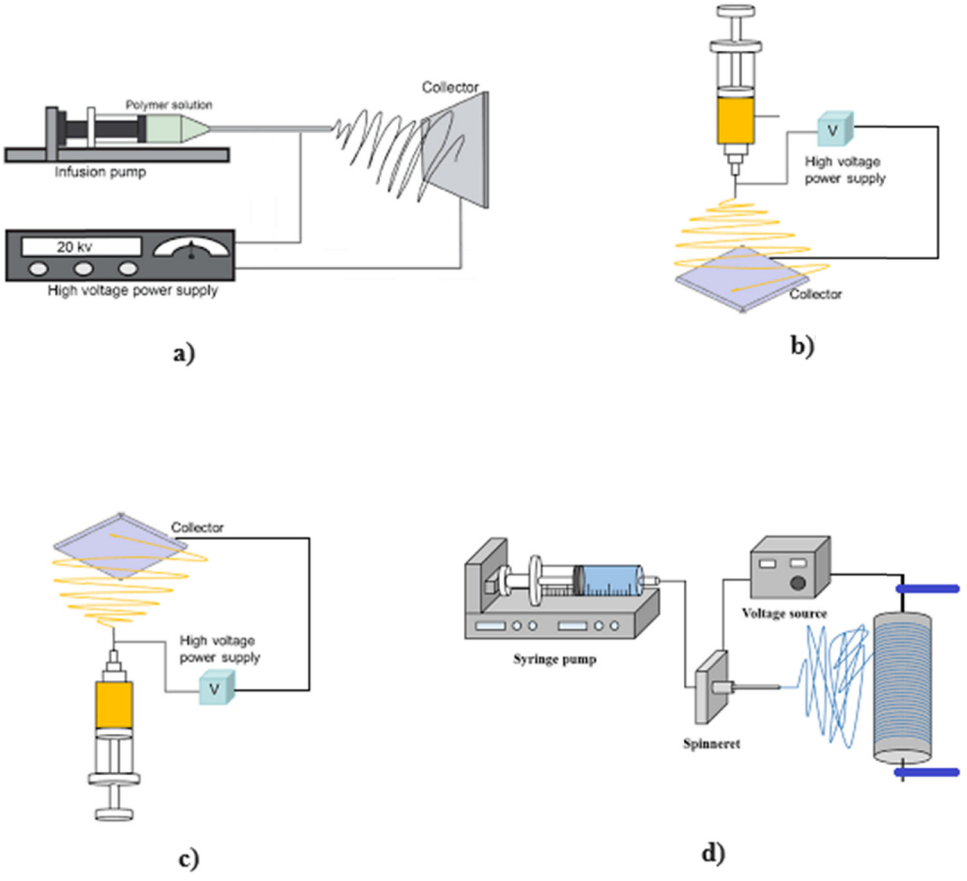

Figure 1: Common electrospinning configurations. (a) Horizontal, (b) top-down, (c) bottom-up, and (d) rotating drum.

solution, the concentration of lignin solution, electrospinning voltage, electrospinner configuration, feed rate, and the distance between nozzle and collector [20,56–60].

This study aimed to extract lignin sustainably and efficiently from SB and subsequently fabricate LNFs for the fabrication of LCFs. This was achieved via acetosolv MW-assisted lignin extraction from SB. The LNFs were then fabricated in a facile and efficient manner using electrospinning. To the best of our knowledge, this is the first time lignin from SB has been extracted using a fully acetosolv MW-assisted heating method. Avelino et al. extracted lignin from SB using 90% (v/v) AA and 2% HCl in 30 min using an open configuration [42]. In this study, a closed vessel setup was utilised and we managed to achieve extraction within 10 min without using HCl as a catalyst. In addition, we utilised the extracted lignin to make LNFs via an electrospinning process, which is rare for lignin derived from SB. As part of the study, being aware of structural differences between lignin sources (as a result of lignin source and extraction methods used), we sought to determine the virtually unique optimum parameters that would allow the extracted acetosolv lignin from SB to be electrospun into LNF without causing electrosprays. In this regard, we were able to determine the flow rate, voltage, distance between poles and lignin to plasticiser ratio required to successfully achieve the electrospinning of acetosolv lignin from SB into LNFs.

2 Materials and methods

All chemicals were purchased from commercial sources and were used as received without further purification at analytical grade. SB was procured from the Council for Scientific and Industrial Research in Durban, South Africa.

2.1 MW-assisted acetosolv extraction of lignin from SB

Sugarcane bagasse (SB) was dried overnight at 105°C in a convection oven and sieved with a 1 mm sieve. The powder was collected into a zip-lock bag and stored in a desiccator. The MW-assisted extraction of lignin from SB was carried out in triplicate.

About 1.0 g of SB was weighed into a 35 mL glass MW vial and 20 mL of pure AA (99.5% v/v) was added; after that, a stirrer bar was dropped in. The vial was placed in an MW synthesiser (CEM discover SP model number 909155) set at 120°C for 10 min with a ramp time of 3 min.

Upon completion, a dark brown solution with a residue at the bottom was observed. The residue was filtered using a Buchner funnel. After that, the residue in the Buchner funnel was washed three times using 10 mL of AA. The dark brown filtrate was transferred to a 100 mL round bottom flask and placed in a rotary evaporator to remove the AA solvent to approximately 5 mL. About 40 mL of distilled water was added dropwise while stirring, resulting in the precipitation of dark brown lignin solid. The mixture was centrifuged at 4,000 rpm for 10 min. The brown SB-derived lignin (SBL) was then filtered on a Buchner funnel, washed five times with 10 mL of water, and subsequently dried under vacuum overnight, weighed, and stored in a glass vial.

2.2 Conventional acetosolv extraction of lignin from SB

The conventional extraction of lignin from SB was conducted in an autoclave. The extraction was carried out in triplicate. The reaction conditions were set at a temperature of 120°C for 10 min, with a ramp time of 10 min. After the reaction, the vessel was left to cool down naturally to reach room temperature.

Upon completion, a dark brown solution with some residue was observed. The mixture was separated using a Buchner funnel. The residue in the funnel was washed three times using 10 mL of AA. The dark brown filtrate was transferred to a 100 mL round bottom flask and placed in a rotary evaporator to reduce the AA solvent to approximately 5 mL. After that, 40 mL of distilled water was added dropwise while stirring, resulting in the precipitation of a dark brown solid (lignin). The mixture was centrifuged at 4,000 rpm for 10 min. The brown SBL was then filtered on a Buchner funnel, washed five times with 10 mL of water, dried under vacuum overnight, weighed, and stored in a glass vial.

2.3 Electrospinning of LNFs

A 10% (w/w) solution of an 85/15% w/w lignin/poly(ethylene oxide) (PEO) blend was made by dissolving 170 mg of SBL and 30 mg of PEO (200,000 $g{\cdot}mol^{-1}$) in 1.8 g of DMF. After dissolution, the mixture was magnetically stirred for 2 h and then left to stand for another 2 h. Electrospinning was conducted using a Nanospinner-1 (Basic System) Single Nozzle Electrospinning Machine (Turkey) with a voltage range of 0–40 kV. A 1 mL syringe of 4 mm diameter was used at a flow rate of 0.3 $mL{\cdot}h^{-1}$,

20 kV voltage, and a distance of 10 cm from the negative plate. Nanofibres were collected on an aluminium foil placed on the negative plate. The nanofibres were placed in a vial, sealed, and subjected to transmission electron microscopy (TEM) analysis.

2.4 Characterisation

For pyrolysis gas chromatography with mass spectrometry (Py-GC/MS), approximately 100–150 µg of the sample were pyrolysed at 550°C for 20 s and the interface temperature to the analytical column was set at 350°C. The samples were analysed by Py-GC/MS detection using a multi-shot pyroliser, EGA/PY-3030 D (Frontier Lab, Japan) attached to a Shimadzu gas chromatograph/mass spectrometer (QP2010 SE). The chromatographic separation of the pyrolysis products was performed using an ultra-alloy capillary column (Frontier Lab, Japan) (30 m × 0.25 mm, 0.25 µm). The injection temperature was set to 280°C and the column flow rate was set to 1.0 mL·min^{-1} with helium used as a carrier gas. The GC temperature programme used was as follows: (i) held at 50°C for 2 min, (ii) ramped from 50°C to 200°C at a rate of 5°C·min^{-1}, and (iii) then held for a further 18 min. The ion source and interface temperatures in the mass spectrometer were set to 200°C and 300°C, respectively. The scan range used for the mass selective detector was from m/z 40 to 650. The pyrolysis products were identified by comparing their mass spectra with the mass spectra in NIST 14 and Wiley 10 databases.

For thermogravimetric analysis (TGA), about 12.6 mg of the respective lignin sample was weighed in the pan for the analysis. The oven was programmed from 30°C to 900°C at a constant heating rate of 10°C·min^{-1}, then held at 900°C for 5 min. Nitrogen (N_2) at a 20 mL·min^{-1} flow was used to prevent any probable air combustion of the lignin sample. TGA data were collected on a Perkin Elmer STA 6000 machine (USA).

Heteronuclear single quantum coherence nuclear magnetic resonance HSQC NMR data were collected on a Bruker Avance 400 MHz spectrometer (Germany). HSQC NMR spectra were obtained under ambient conditions in DMSO-d_6 deuterated solvent. NMR data are expressed in parts per million (ppm).

A JEOL 1010 (Japan) transmission electron microscope (TEM) was used to characterise the morphology and size of the produced LNFs.

Infrared spectra were obtained at ambient temperature on a Fourier transform infrared (FTIR) spectroscope (Perkin Elmer Spectrometer, Model 100, USA) equipped with a universal ATR sampling accessory. All characteristic peaks are reported in wavenumbers (cm^{-1}) in the range of 4,000–400 cm^{-1}.

For size exclusion chromatography (SEC), the DMAc system consisted of a Shimadzu LC-10AD pump, a Waters in-line degasser AF, and a Waters 717plus autosampler (Japan). A Waters 2487 dual wavelength UV and a Waters 410 differential refractive index were connected in series as detection systems. Dimethyl acetamide (DMAc, HPLC grade, stabilised with 0.05% BHT and 0.03% LiCl) was used as mobile phase at 40°C and a flow rate of 1 mL·min^{-1}, and the system was calibrated using narrow poly(methylmethacrylate) standards ranging from 634 to 1.944 × 10^6 g·mol^{-1}. The column set included a 50 mm × 8 mm guard column in series with three 300 mm × 8 mm, 10 µm particle size GRAM columns (two 3,000 Å and a 100 Å) obtained from Polymer Standards Service. Concentration in DMAc was set at 1,000 g·L^{-1}.

The polydispersity index (PDI) was calculated using the following formula:

$$\mathrm{PDI} = \frac{M_\mathrm{w}}{M_\mathrm{n}} \tag{1}$$

3 Results and discussion

3.1 Extraction

The MW extraction of lignin from SB required no special preparation. In this study, lignin was extracted using 100% (v/v) AA at 120°C in a sealed MW vial after 10 min, without the need for a mineral acid catalyst. This setup was more efficient compared to a similar extraction of lignin by others from SB, which used 90% v/v AA and 2% v/v of HCl at 110°C in 30 min in an open reflux system [42]. The sealed vial used here encouraged the build-up of pressure in the vessel, which aided in the rupture of cell walls to release the lignin [61]. To improve sustainability, the AA used in SBL extractions was recycled and used in other extractions once removed using a rotary evaporator. The hydrophobic nature of the acetosolv SBL produced enabled easy separation from the residual AA solution, as precipitation was readily achieved by simply adding water. This ensured a green extraction of lignin from SB without the use of toxic chemicals or needless wastage of solvents.

AA was chosen due to several factors: it has a high solubility of lignin, which allowed for lignin's easy extraction and separation from the AA insoluble cellulose in the SB [62]. In addition, AA is an MW-responsive solvent due to its polar nature, ensuring adequate MW absorption during MW extraction of lignin from SB. AA is also a relatively cheap organic acid that is environmentally benign,

especially compared to mineral acids such as sulphuric acid [63]. Additionally, AA can be produced from the oxidation of ethanol derived from biomass [37], which can, in turn, encourage a circular economy at potential bio-refineries.

Several factors were optimised during lignin extraction (Figure 2), such as temperature, reaction duration, and AA concentration. These were optimised to an AA concentration of 100% v/v, at a temperature of 120°C for 10 min. The optimised MW conditions were then used in a conventional heating method using an autoclave for comparison. The MW-assisted method took approximately 20 min in total for the ramp-up time, the actual reaction, and the cooling period combined. However, the autoclave required approximately 1 h in total due to its slower heating rate and extended cooling period. The MW-assisted method had an average lignin yield of 205 mg, while the conventional method had an average yield of 183 mg.

MW-assisted heating is generally known to be more time, energy, and process efficient compared to conventional heating due to its volumetric heating [64–67]. Because fossil fuels that are often used for energy production have adverse environmental effects [68], MW-assisted heating is, therefore, inherently more environmentally friendly by being energy efficient [69]. MW-assisted heating can also be turned on and off instantaneously, allowing for better process control. The shorter reaction time due to increased processing efficiency allows for a smaller vessel that takes less space to be used to produce the same amount of products as a larger conventional heated vessel would [70].

While MW-assisted heating proved to be an energy and time-efficient technology useful in process intensification because of its rapid volumetric heating when compared to conventional heating, it has not been implemented in the chemical industry on a larger scale. The capital-intensive nature of retrofitting MW reactors onto existing bio-refineries can perhaps not be economically justified by the improvement in efficiency due to MW. In addition to health and safety, concerns regarding MW radiation exposure and also explosion risks are associated with the fast heating rates and the rapid build-up of pressure in vessels.

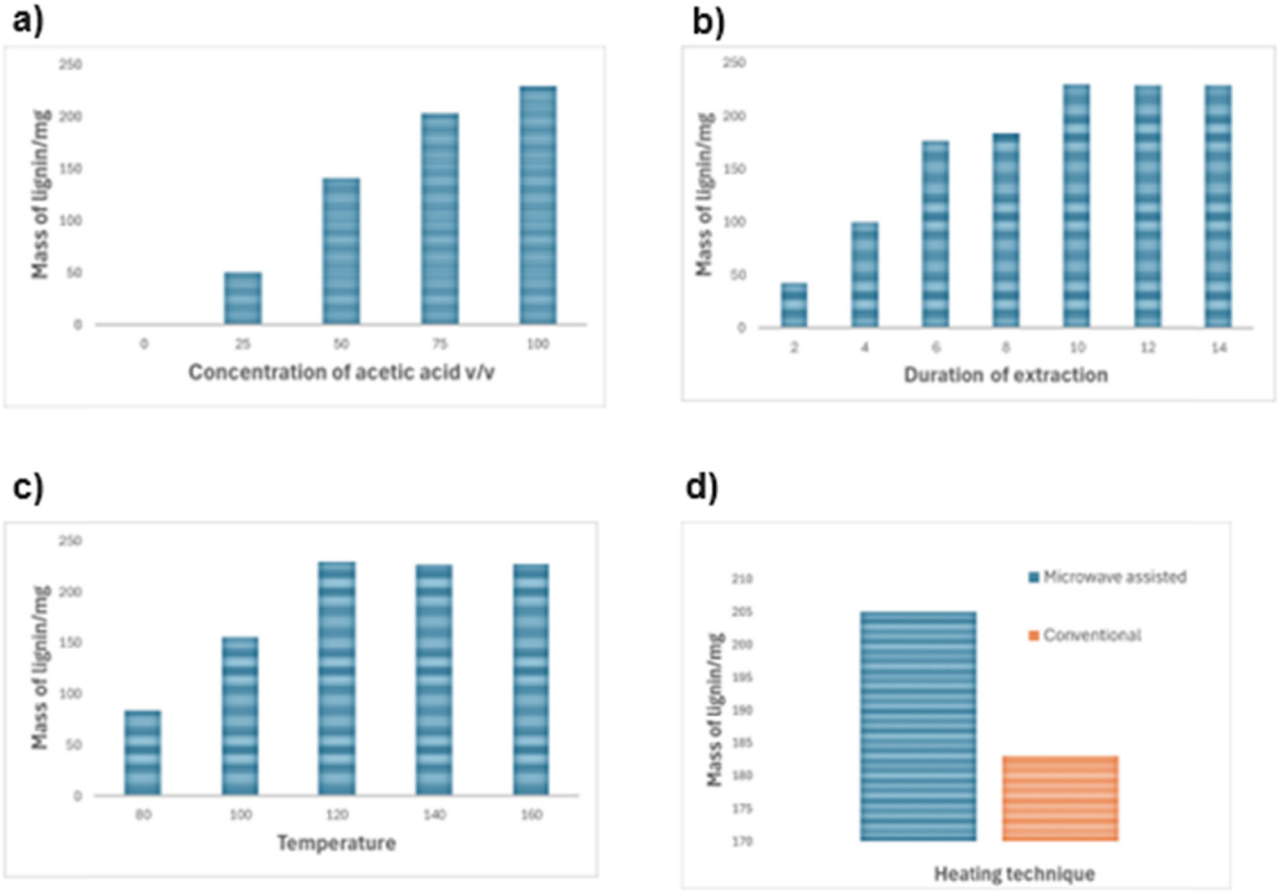

Figure 2: Effect of different parameters on the extraction yield of lignin from sugarcane bagasse using MW-assisted heating. (a) MW at 160°C, 12 min and AA concentration 0%, 25%, 50%, 75%, and 100% (v/v). (b) MW at 160°C, AA concentration 100% (v/v), 2–14 min. (c) MW at AA concentration 100% (v/v), 10 min, 80–160°C. (d) MW versus conventional heating, 120°C, 10 min, 100% (v/v).

The proper techno-economic analysis of the economic viability of the extraction of MW lignin requires quantitative scale-up models, which can be used to predict the behaviour of MW heating at a larger scale. A computational study of general MW-assisted heating by Goyal et al. predicted an eventual decrease in the energy absorbed as the vessel size increased [71]. Penetration limitations of MW radiation could produce coldspots and hotspots within larger vessels, and multiple MW generators (magnetrons) could be fitted to strategic positions to ensure even heating within the vessel if technically feasible. It would be interesting to investigate using a computational study how multiple magnetrons would improve the challenges identified.

3.2 Electrospinning of lignin fibres

Attempts to replicate the experimental electrospinning conditions set by Wang and co-workers [72] using organosolv (Alcell) lignin were unsuccessful, likely due to structural differences between the different lignin sources used, a result of different lignin extraction methods used that inadvertently altered the lignin structure [27,73] and differences in monolignol composition (H/G/S ratio) [74]. These differences, in turn, altered the rheological properties of the spinning solution used, even though both lignins used were organosolv lignins. New parameters had to be determined to enable the SBL to be electrospun without sputtering and producing electrosprays [75] by optimising the lignin/PEO ratio, the distance from the collecting plate and the voltage, among other parameters. This highlights the need to investigate the optimal electrospinning parameters for each unique lignin source to enable various lignin sources to be efficiently electrospun into LNFs.

The starting parameters used for this electrospinning were replicated from the work done by Wang and co-workers [72] using organosolv (Alcell) lignin. Initially, a 90/10% w/w lignin/PEO in DMF solution at a flow rate of 0.3 $mL{\cdot}h^{-1}$ at 6.5–7.0 kV and a needle tip-to-plate substrate distance of 10 cm was used. The voltage was increased in 1 kV increments until 20 kV, which induced a Taylor cone, a polymer jet, and the resultant electrospray of the polymer solution onto the collecting plate. This formation of droplets instead of fibres implied that the solution lacked enough plasticity to be spun into fibres. The concentration of the PEO plasticiser was therefore increased from 10% w/w to 15% w/w before jets of the polymer solution began to form electrospun fibres on the collecting plate. The conditions that enabled electrospinning to occur were determined as an 85%/15% w/w lignin/PEO solution in DMF at 20 kV, 10 cm distance, and flow rate of 0.3 $mL{\cdot}h^{-1}$.

Electrospinning LNFs from neat lignin alone is challenging, attributable to molecular weight distribution, cross-linking and intermolecular interaction within the lignin framework. Ideally, narrower molar mass distributions to obtain viscous flow and fibre formation when dissolved in solvents are desirable [19]. Small amounts of a second high MW polymer acting as a plasticiser are often required for electrospinning to occur, as pure lignin solutions typically produce electrosprays rather than be drawn into fibres. Common plasticisers include PAN [76], poly(vinyl alcohol), or PEO [72]. The inclusion of these synthetic polymers is often necessary to improve the lignin solution's rheological properties and promote fibre formation. The addition of a plasticiser is believed to cause the formation of hydrogen bonds with the hydroxyl groups of the lignin [77], which provides the necessary chain entanglement (Figure 3) [78,79]. Incorporation of renewable natural biopolymers such as poly(lactic acid) [80,81], cellulose [82], and poly(hydroxybutyrate [80] for

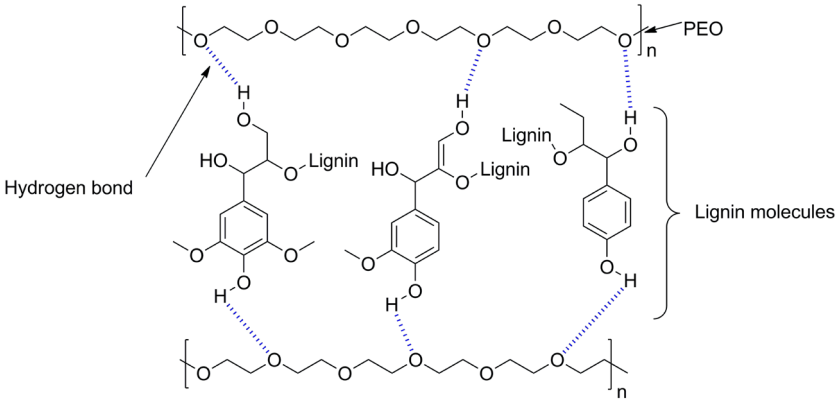

Figure 3: The formation of hydrogen bonds between PEO and lignin molecules to improve plasticity and promote fibre formation during electrospinning.

greener fibre formation is ultimately imperative for more sustainable production of electrospun LNFs.

Good reproducibility in electrospun fibre characteristics across batches could be affected by variations in relative humidity and ambient temperature in response to prevailing weather conditions [83], necessitating the need for air-conditioned rooms. Slight variations in lignin structure can also be anticipated when using lignin from different sugarcane varieties, and different breeds and hybrids are grown depending on the region. These differences may alter the electrospinning conditions that are optimal for particular LNF characteristics [84].

3.3 Characterisation of lignin and LNFs

3.3.1 SEC

SBL was characterised using SEC to determine the average molecular weight (M_w) and the number average molecular weight (M_n) of the lignin and its fragments to determine its molecular size using the average molecular weight and evaluate the distribution of its fragments [85]. An M_w of 12,124 g·mol^{-1} and M_n of 5,655 g·mol^{-1} were determined and a PDI of 2.14 was calculated. Figure 4 shows the molar mass distribution curve of SBL.

3.3.2 FTIR spectroscopy

Lignin is a complex amorphous polymer, and the theoretical data assignment is inherently challenging because of the overlap of multiple vibration modes from numerous different functional groups within lignin, particularly below 1,400 cm^{-1}. The band assignments in lignin were accomplished based on the characteristic absorption bands of moieties in the lignin skeleton using data from various lignin model compounds and lignins published in previous reports [27,86–92]. Figure 5 shows the FTIR spectrum for SBL, and Table 1 shows selected absorption bands. Absorptions attributed to the lignin's three common monolignol units were observed and anticipated, given the herbaceous nature of SB [88]. The bands at 1,604, 1,510, and 1,427 cm^{-1} were assigned to the aromatic ring stretching mode [87,88,90–92], suggesting that the aromatic structures of the selected lignins remained reasonably unaffected by the MW-assisted AA extraction process. In particular, the bands at 1,322 and 1,113 cm^{-1} were assigned to characteristic syringyl (S) units [87,91,92], while the band at 1,026 cm^{-1} was attributed to the presence of guaiacyl (G) units [91], and the C–H out of a plane in the *p*-hydroxyphenyl propane units (H) were at 836 cm^{-1}. The band at 3,396 cm^{-1} was ascribed to the O–H stretching signal of hydrogen-bonded hydroxyl groups in the aliphatic and aromatic sections of lignin's structure, respectively [92]. The C–H stretch in methyl and methylene groups was at 2,934 cm^{-1} [91,92]. The bands at 2,854 cm^{-1} also corresponded to the C–H stretching in methylene, methyl, and methoxy groups.

3.3.3 HSQC NMR

The macromolecular structure of the SBL was studied further using HSQC; this important tool was used to establish the structure of lignin by providing detailed information on the various types of hydrogen and carbon atoms,

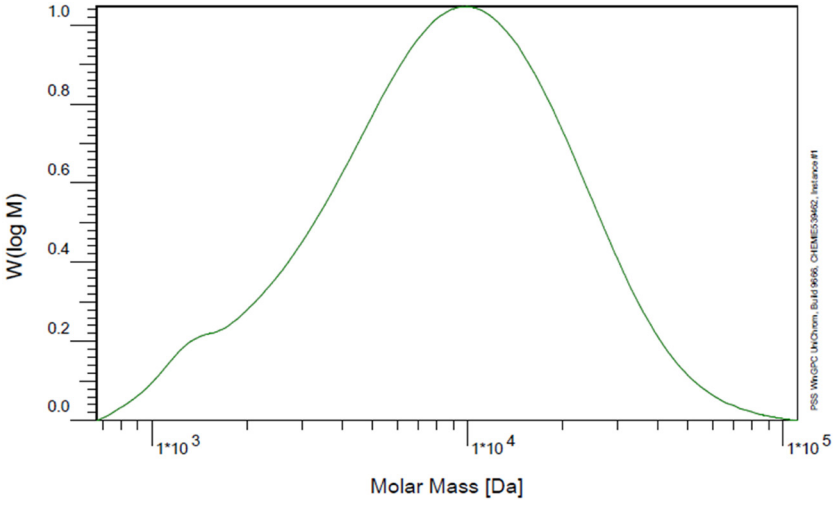

Figure 4: Molar mass distribution curves of SBL.

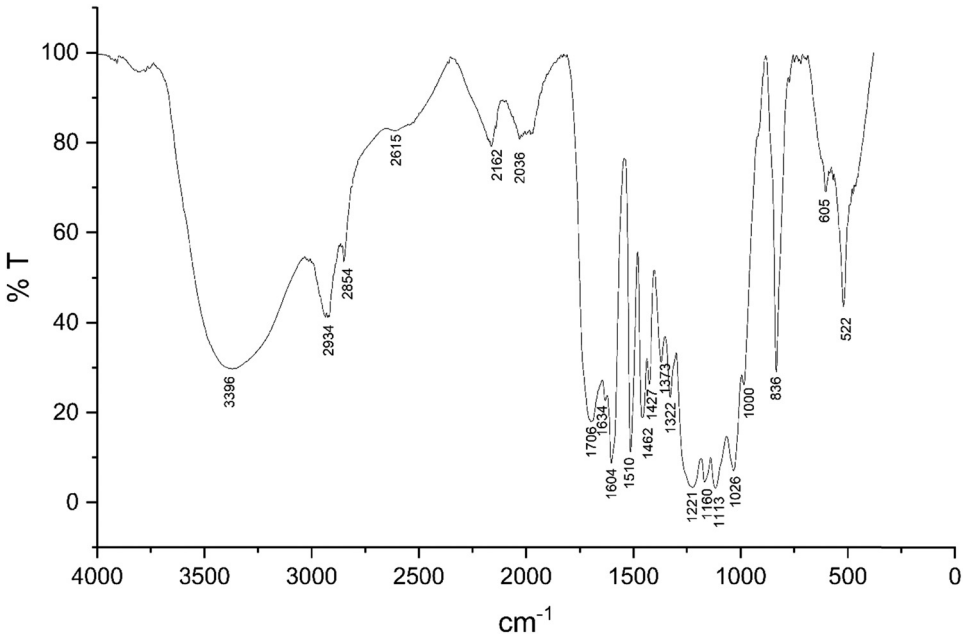

Figure 5: FTIR spectrum of SBL.

Table 1: Selected FTIR signals and band assignments

Peak (cm^{-1})	Band assignment
3,396	Phenolic and aliphatic O–H stretching
2,934	C–H stretching in methyl, methylene, or methane group
2,854	C–H stretching in methyl, methylene, or methoxy group
1,706	C═O stretch in unconjugated carbonyl groups, carbonyl and ester groups, or LCC
1,634	C–O stretch in conjugated ketone
1,604	C–C stretching (aromatic skeleton)
1,510	C═C stretching (aromatic skeleton)
1,462	C–H deformation (asymmetric in CH_3 and CH_2)
1,427	C–C stretching (aromatic skeleton) with C–H in plane deformation
1,373	Aliphatic C–H stretch in CH_3
1,322	Syringyl ring breathing with C–O stretching
1,221	Aromatic C–O stretching
1,160	C–O stretch in ester groups
1,113	Aromatic C–H in-plane deformation for syringyl type
1,026	Aromatic C–H in-plane deformation for guaiacyl type
836	C–H out of plane in the *p*-hydroxyphenyl propane units

confirming the presence of functional groups and types of linkages in the lignin sample used for analysis [92]. Notable chemical functionalities were assigned based on the various lignin model compounds from a variety of reports and databases [27,42,92–95]. Figure 6 shows the HSQC spectrum for SBL.

In lignin studies using HSQC, particular moieties are found in certain regions. The aliphatic side chain is at chemical shift (δ) = 0.5–2.8 ppm, aliphatic oxygenated side chain δ = 2.5–5.8 ppm, the aromatic groups δ = 5–8.5 ppm, and the aldehyde functional group δ = 9–10 ppm. The signals at 0.83, 1.22, 1.45, and 1.94 ppm were assigned to aliphatic groups of lignin. The DMSO-d_6 solvent residual signal was at 2.5 ppm [95]. The significant peak overlap from an intense broad peak from 2.80 to 3.85 ppm was attributed to the presence of lignin carbohydrate complexes (LCCs) in the form of cellulose and hemicellulose derivatives in the SBL sample [96]. The presence of signals associated with the 3 main monolignols (H/G/S) corroborated the FT-IR data. The signals at δ_C/δ_H 103.2/6.65, 116.3/6.27, and 116.3/6.77 were attributed to G and/or S units of lignin, and the presence of either G or S units was also substantiated by the cross-peak at δ_C/δ_H 55.8/3.7 associated with the methoxy group (–OCH_3), which can be found on 3/5 positions on G or S units. The correlations at δ_C/δ_H 145.3/7.42, 145.8/7.34, and 131.78/7.50 were associated with the *p*-hydroxyphenyl (H) unit, which was the furthest downfield signal observed in the HSQC spectrum.

3.3.4 Py-GC-MS

Py-GC-MS was used to elucidate the structure of lignin in more detail, and the phenolic compounds were determined based on their retention times and compared to a database.

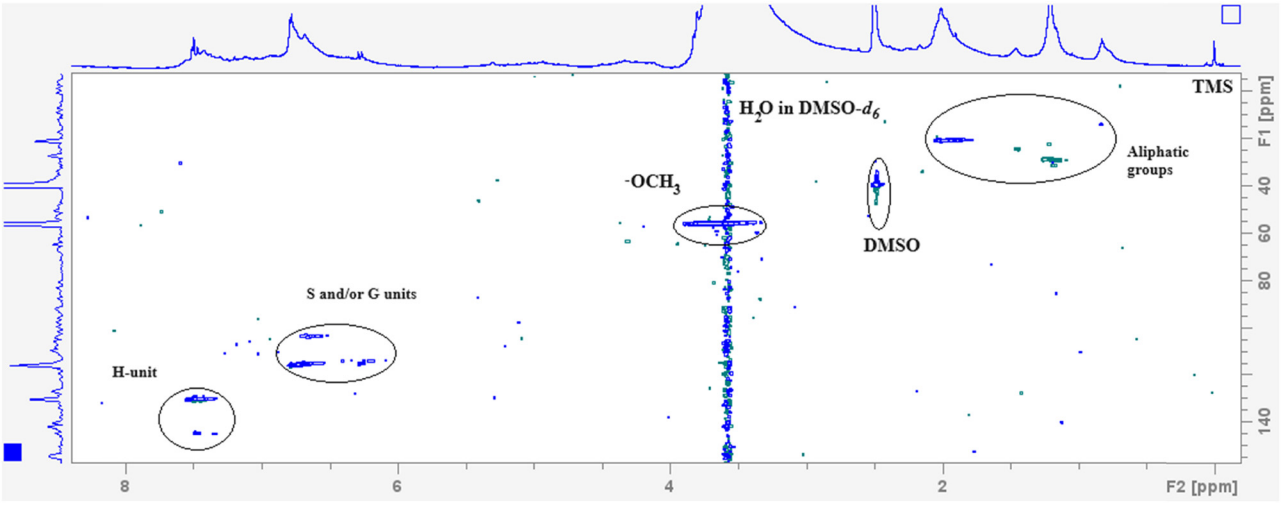

Figure 6: HSQC spectrum of SBL displaying chemical shifts and suggested assignments.

This analysis confirmed lignin markers derived from H, S, and G phenylpropanoid units in SB and gave an insight into SBL's monolignol composition, as suggested by FT-IR and NMR data, although we did not go into greater detail regarding the H:G:S ratio. The py-GC-MS spectrum is shown in Figure S1. From the compounds observed in the spectrum, they maintained their ring substitution patterns from the lignin polymer and could be identified and grouped as being derived from the *p*-hydroxyphenyl (H), guaiacyl (G), or syringyl (S) units [88].

Table 2 shows the ten most abundant aromatics assigned to their perceived monolignol origin in descending order of their abundance. Most of the compounds were predominantly H type, followed by G-type compounds, while there was only one S-type compound. The data can be interpreted as a measure of the dominance of H-type monolignols in the lignin, as inferred by Klein et al. [88]. Alternatively, the thermally induced fragmentation of S-type fragments could have been demethoxylated into G and H monolignols, while G types were converted into H types, resulting in H-type monolignol units' perceived dominance, as depicted in Figure 7.

Table 2: Primary aromatic compounds based on pyr-GC-MS analysis

Percentage area	Compound
6.64*	Benzaldehyde, 2-methyl-
2.97*	2-Propenoic acid, 3-(4-hydroxyphenyl)-, methyl ester
2.33#	1,2-Benzenediol, 4-methyl-
1.9*	Phenol, 4-ethyl-
1.65#	Vanillin
1.57#	2-Methoxy-4-vinylphenol
1.4*	Phenol
1.24*	Benzaldehyde, 4-hydroxy-
1.11&	Benzaldehyde, 4-hydroxy-3,5-dimethoxy-
0.99#	Phenol, 2-methoxy-

Key: *H-type compounds, #G-type compounds, &S-type compounds.

3.3.5 TGA

The thermal properties of the extracted lignin were investigated using TGA, and they provided useful information regarding suitable temperature parameters when applying lignin in the carbonisation of lignin for the fabrication of CFs. The thermal stability of lignin is greatly dependent on its macromolecular structure, molecular weight, inherent chemical linkages, crosslinking degree, and carbohydrate impurity content (as a result of LCCs) [75,97], among other variables, mainly due to the source of lignin and/or its extraction process [98–100].

The thermograms of SBL are shown in Figure 8. The thermogravimetric (TG) thermogram shows the temperature ranges as degradation ensued, the corresponding percentage weight loss, maximum thermal decomposition temperature (DTG_{max}), and percentage residual carbon of the SBL, while the DTG curve signified the rate of weight

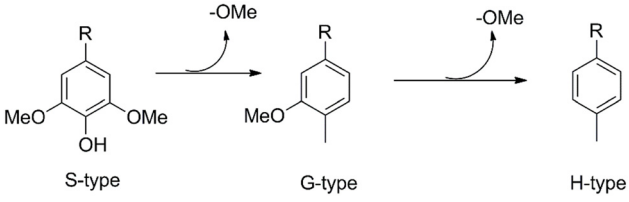

Figure 7: Demethoxylation of S-unit to G-unit and then to H unit.

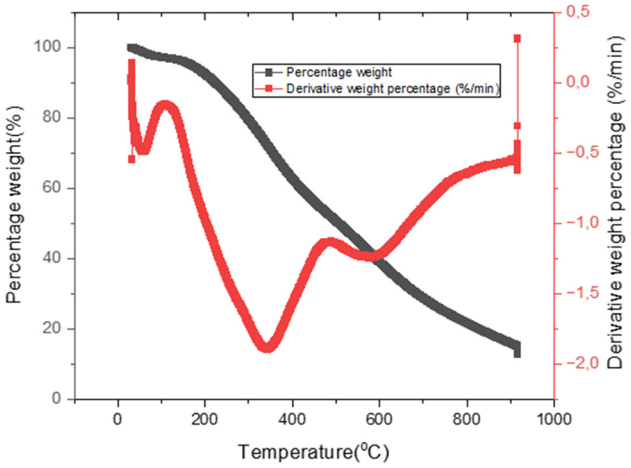

Figure 8: TG, derivative TG, and DSC thermograms of SBL.

loss with temperature. The thermograms displayed three significant thermal events of weight loss as the decomposition of various bonds proceeded, at 60°C, 350°C, and ~600°C, as observed from the decrease in the DTG.

The first stage from ~60°C involves the elimination of solvent/moisture and low molecular weight volatiles in the SBL sample [87,101–103]. Stage 2 occurs around 180–350°C. This is the greatest weight loss, as shown by the DTG curve, which shows the greatest decrease in this region. Decomposition in this stage involves the fragmentation of inter-unit monolignol ether linkages, aliphatic chains, and decarboxylation reactions, transferring monomers and other aromatic derivatives into the vapour phase, partly depending on the differences in the content of C–C [104,105]. The major products of this stage are gaseous products, organic and phenolic products, and coke [87]. The degradation of carbohydrate impurities in lignin samples also occurs, converting them into volatile gases such as CO, CO_2, and CH_4 [27,106]. The third significant degradation occurs after ~600°C, and the process is associated with the decomposition of the stable aromatic rings [107]. The lignin samples are pyrolysed into a highly condensed carbonaceous residue of non-volatilised char [27], with a resultant residual weight of ~10%.

3.3.6 TEM

After the fabrication of LNFs via electrospinning, they were analysed using TEM to determine their general pattern and size (Figure 9). Electrospun LNFs were observed as haphazardly arranged fibres of diameters ~15 nm, forming a mat-like material. The LNFs generated in this study had significantly smaller diameters of about 20 nm compared to ~500 nm collected by Wang et al. using a similar method [72]. The differences in the structure of the lignin (and monolignol proportion) could play a role in this disparity, as well as the differences in the lignin/PEO ratio and the voltage.

4 Conclusions

The MW-assisted extraction of lignin from SB, an underutilised agrowaste, was sustainably and efficiently achieved using AA, within 10 min, without the addition of a mineral acid catalyst. The lignin was subsequently utilised to fabricate LNFs using an electrospinning method, an easy, cheap, and fast production method of fibres, with the ultimate goal of carbonising the LNFs to produce non-structural CFs from SB-derived lignin for application in lithium ion or sodium ion batteries. This displayed the immense potential of SB in the production of more valuable sustainable materials, especially when process intensification methods such as MW-assisted

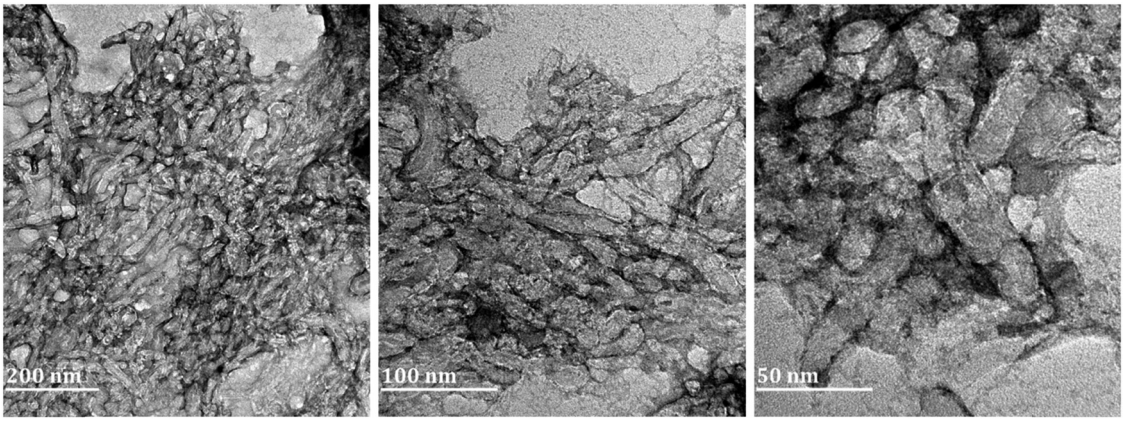

Figure 9: TEM images of the synthesised lignin-PEO blend nanofibres.

heating are used for process efficiency, which can contribute positively to the circular economy and the process economics of typical sugarcane processing biorefineries

During electrospinning, neat acetosolv lignin alone was not electrospinnable; instead, it produced electrosprays. This necessitated the addition of a PEO plasticiser to encourage spinning. An 85/15% w/w lignin/PEO solution in DMF was sufficient to induce electrospinning of the lignin/PEO solution to form a mat of randomly woven nanofibres. We also observed differences in conducive electrospinning parameters to those used by researchers previously in terms of voltage, which necessitated the adoption of new electrospinning parameters after trial and error. The structural differences between the lignin sources were likely responsible for the parameter differences that were conducive for electrospinning.

The application of MW-assisted heating was important in this study as an efficient process intensification technique within industrial, educational, and research spaces. Scaling up of MW processing has been slow despite considerable research output over the years. This could be a result of high equipment cost, which outweigh potential financial gains, after considering the long-term effects on operations and the cost of ownership; an inadequate understanding of the processing limitations involved in MW penetration, health and safety aspects regarding the exposure to large amounts of MW radiation, explosion risks associated with the rapid temperature increase and pressure build-up. The development of safe, robust, and scalable MW-assisted reaction vessels calls for an intimate alliance among multidisciplinary researchers and equipment manufacturers.

Acknowledgements: We thank the School of Chemistry and Physics, University of KwaZulu-Natal (UKZN), South Africa, for financial support and facilities, and the research supported by the Eskom TESP Program (P677), and in part by the National Research Foundation of South Africa (Grant Number: 132014).

Funding information: The research was supported by the Eskom TESP Program (P677), and in part by the National Research Foundation of South Africa (Grant Number: 132014).

Author contributions: Emmanuel Mkumbuzi: conceptualisation, visualisation, writing – original draft, writing – review and editing. Bishop Bruce Sithole: review and editing. Werner Ewald van Zyl: conceptualisation, writing – review and editing, supervision and finances.

Conflict of interest: Authors state no conflict of interest.

Data availability statement: Data sharing is not applicable to this article as no datasets were generated or analysed during the current study.

References

[1] Church D. A revolution in low-cost carbon fiber production. ReinPlast. 2018;62(1):35–7. doi: 10.1016/j.repl.2017.11.003.

[2] Hosseinaei O, Harper DP, Bozell JJ, Rials TG. Improving processing and performance of pure lignin carbon fibers through hardwood and herbaceous lignin blends. Int J Mol Sci. 2017;18(7):1410. doi: 10.3390/ijms18071410.

[3] Choi D, Kil HS, Lee S. Fabrication of low-cost carbon fibers using economical precursors and advanced processing technologies. Carbon. 2019;142:610–49. doi: 10.1016/j.carbon.2018.10.028.

[4] Strassberger Z, Tanase S, Rothenberg G. The pros and cons of lignin valorisation in an integrated biorefinery. RSC Adv. 2014;4(48):25310–8. doi: 10.1039/c4ra04747h.

[5] Toscano Miranda N, Lopes Motta I, Maciel Filho R, Maria RWM. Sugarcane bagasse pyrolysis: A review of operating conditions and products properties. Renew Sustainable Energy Rev. 2021;149(June):111394. doi: 10.1016/j.rser.2021.111394.

[6] Sen KY, Baidurah S. Renewable biomass feedstocks for production of sustainable biodegradable polymer. Curr Opin Green Sustain Chem. 2021;27:100412. doi: 10.1016/j.cogsc.2020.100412.

[7] Pan S, Zabed HM, Wei Y, Qi X. Technoeconomic and environmental perspectives of biofuel production from sugarcane bagasse: Current status, challenges and future outlook. Ind Crops Prod. 2022;188(PB):115684. doi: 10.1016/j.indcrop.2022.115684.

[8] Varshney D, Mandade P, Shastri Y. Multi-objective optimization of sugar- cane bagasse utilization in an Indian sugar mill. Sustain Prod Consum. 2019;18:96–114. doi: 10.1016/j.spc.2018.11.009.

[9] Negrão DR, Grandis A, Buckeridge MS, Rocha GJM, Leal RLV, Driemeier C. Inorganics in sugarcane bagasse and straw and their impacts for bioenergy and biorefining: A review. Renew Sustainable Energy Rev. 2021;148(September 2020):11268. doi: 10.1016/j.rser.2021.111268.

[10] Peuvot K, Hosseinaei O, Tomani P, Zenkert D, Lindbergh G. Lignin based electrospun carbon fiber anode for sodium ion batteries. J Electrochem Soc. 2019;166(10):A1984–90. doi: 10.1149/2.0711910jes.

[11] Shi X, Wang X, Tang B, Dai Z, Chen K, Zhou J. Impact of lignin extraction methods on microstructure and mechanical properties of lignin-based carbon fibers. J Appl Polym Sci. 2018;135(10):1–7. doi: 10.1002/app.45580.

[12] Wang S, Li Y, Xiang H, Zhou Z, Chang T, Zhu M. Low-cost carbon fibers from bio-renewable Lignin/Poly(lactic acid) (PLA) blends. Compos Sci Technol. 2015;119:20–5. doi: 10.1016/j.compscitech.2015.09.021.

[13] Jayawickramage P, Rangana A, Ferraris JP. High performance supercapacitors using lignin-based electrospun carbon nanofiber electrodes in ionic liquid electrolytes. Nanotechnology. 2019;30(15):155402. doi: 10.1088/1361-6528/aafe95.

[14] García-Mateos FJ, Ruiz-Rosas R, María Rosas J, Morallon E, Cazorla-Amorós D, Rodríguez-Mirasol J. Activation of electrospun lignin-based carbon fibers and their performance as self-standing supercapacitor electrodes. Sep Purif Technol. 2020;241(February):116724. doi: 10.1016/j.seppur.2020.116724.
[15] Schlee P, Herou S, Jervis R, Shearing PR, Brett DJL, Baker D. Free-standing supercapacitors from Kraft lignin nanofibers with remarkable volumetric energy density. Chem Sci. 2019;10(10):2980–8. doi: 10.1039/c8sc04936j.
[16] Jia H, Sun N, Dirican M, Li Y, Chen C, Zhu P. Electrospun kraft lignin/cellulose acetate- derived nanocarbon network as an anode for high-performance sodium-ion batteries. ACS Appl Mater Interfaces. 2018;10(51):44368–75. doi: 10.1021/acsami.8b13033.
[17] Shi Z, Jin G, Wang J, Zhang J. Free-standing, welded mesoporous carbon nanofibers as anode for high-rate performance Li-ion batteries. J Electroanal Chem. 2017;795:26–31. doi: 10.1016/j.jelechem.2017.03.047.
[18] Ma X, Smirnova AL, Fong H. Flexible lignin-derived carbon nanofiber substrates functionalized with iron (III) oxide nanoparticles as lithium-ion battery anodes. Mater Sci Eng B Solid-State Mater Adv Technol. 2019;241(January):100–4. doi: 10.1016/j.mseb.2019.02.013.
[19] Khan I, Hararak B, Fernando GF. Improved procedure for electrospinning and carbonisation of neat solvent-fractionated softwood Kraft lignin. Sci Rep. 2021;11(1):1–13. doi: 10.1038/s41598-021-95352-5.
[20] Li W, Li M, Adair KR, Sun X, Yu Y. Carbon nanofiber based nanostructures for lithium-ion and sodium-ion batteries. J Mater Chem A. 2017;5(27):13882–906. doi: 10.1039/c7ta02153d.
[21] Svinterikos E, Zuburtikudis I, Al-Marzouqi M. Electrospun lignin-derived carbon micro- and nanofibers: a review on precursors, properties, and applications. CS Sustain Chem Eng Published. 2020;8:13868–93. doi: 10.1021/acssuschemeng.0c03246.
[22] Beck RJ, Zhao Y, Fong H, Menkhaus TJ. Electrospun lignin carbon nanofiber membranes with large pores for highly efficient adsorptive water treatment applications. J Water Process Eng. 2017;16:240–8. doi: 10.1016/j.jwpe.2017.02.002.
[23] Nordin NA, Rahman NA, Abdullah AH. Effective removal of Pb(II) ions by electrospun PAN/Sago lignin-based activated carbon nanofibers. Molecules. 2020;25:3081. doi: 10.3390/molecules25133081.
[24] Du B, Liu C, Wang X, Han Y, Guo Y, Li H, et al. Renewable lignin-based carbon nanofiber as Ni catalyst support for depolymerization of lignin to phenols in supercritical ethanol/water. Renew Energy. 2020;147:1331–9. doi: 10.1016/j.renene.2019.09.108.
[25] García-Mateos FJ, Berenguer R, Valero-Romero MJ, Rodríguez-Mirasol J, Cordero T. Phosphorus functionalization for the rapid preparation of highly nanoporous submicron-diameter carbon fibers by electrospinning of lignin solutions. J Mater Chem A. 2018;6(3):1219–33. doi: 10.1039/c7ta08788h.
[26] Paone E, Tabanelli T, Mauriello F. The rise of lignin biorefinery. Curr Opin Green Sustain Chem. 2020;24:1–6. doi: 10.1016/j.cogsc.2019.11.004.
[27] Amit TA, Roy R, Raynie DE. Thermal and structural characterization of two commercially available technical lignins for potential depolymerization via hydrothermal liquefaction. Curr Res Green Sustain Chem. 2021;4(May):100106. doi: 10.1016/j.crgsc.2021.100106.
[28] Laurichesse S, Avérous L. Chemical modification of lignins: Towards biobased polymers. Prog Polym Sci. 2014;39(7):1266–90. doi: 10.1016/j.progpolymsci.2013.11.004.
[29] Figueiredo P, Lintinen K, Hirvonen JT, Kostiainen MA, Santos HA. Properties and chemical mod- ifications of lignin: Towards lignin-based nanomaterials for biomedical applications. Prog Mater Sci. 2018;93:233–69. doi: 10.1016/j.pmatsci.2017.12.001.
[30] Duval A, Lawoko M. A review on lignin-based polymeric, micro- and nano-structured materials. React Funct Polym. 2014;85(September):78–96. doi: 10.1016/j.reactfunctpolym.2014.09.017.
[31] Zhou L, Budarin V, Fan J, Sloan R, Macquarrie D. Efficient method of lignin isolation us- ing microwave-assisted acidolysis and characterization of the residual lignin. ACS Sustain Chem Eng. 2017;5:3768–74. doi: 10.1021/acssuschemeng.6b02545.
[32] Gan MJ, Niu YQ, Qu XJ, Zhou CH. Lignin to value-added chemicals and advanced materials: extraction, degradation, and functionalization. Green Chem. 2022;24(20):7705–50. doi: 10.1039/d2gc00092j.
[33] Antunes F, Mota IF, da Silva Burgal J, Pintado M, Costa PS. A review on the valorization of lignin from sugarcane by-products: From extraction to application. Biomass and Bioenergy. 2022;166(November):106603. doi: 10.1016/j.biombioe.2022.106603.
[34] Chen M, Li Y, Liu H, Zhang D, Shi QS, Zhong XQ, et al. High value valorization of lignin as environmental benign antimicrobial. Mater Today Bio. 2023;18(December 2022):100520. doi: 10.1016/j.mtbio.2022.100520.
[35] Zhang K, Pei Z, Wang D. Organic solvent pretreatment of lignocellulosic biomass for biofuels and biochemicals: A review. Bioresour Technol. 2016;199:21–33. doi: 10.1016/j.biortech.2015.08.102.
[36] Chen Y, Yang Y, Liu X, Shi X, Wang C, Zhong H, et al. Sustainable production of formic acid and acetic acid from biomass. Mol Catal. 2023;545(April):113199. doi: 10.1016/j.mcat.2023.113199.
[37] Morales-Vera R, Crawford J, Dou C, Bura R, Gustafson R. Techno-economic analysis of producing glacial acetic acid from poplar biomass via bioconversion. Molecules. 2020;25(18):1–16. doi: 10.3390/molecules25184328.
[38] Dalena F, Senatore A, Iulianelli A, Di Paola L, Basile M, Basile A. Ethanol from biomass: Future and perspectives. In: Angelo B, Iulianelli A, Dalena F, Veziroğlu TN, editors. Ethanol: Science and Engineering. Amsterdam: Elsevier; 2018. p. 25–59.
[39] Rajeswari S, Baskaran D, Saravanan P, Rajasimman M, Rajamohan N, Vasseghian Y. Production of ethanol from biomass – Recent research, scientometric review and future perspectives. Fuel. 2022;317(November 2021):123448. doi: 10.1016/j.fuel.2022.123448.
[40] Budsberg E, Morales-Vera R, Crawford JT, Bura R, Gustafson R. Production routes to bio-acetic acid: life cycle assessment. Biotechnol Biofuels. 2020;13(1):1–15. doi: 10.1186/s13068-020-01784-y.
[41] Zhou S, Liu L, Wang B, Xu F, Sun R. Microwave-enhanced extraction of lignin from birch in formic acid: Structural characterization and antioxidant activity study. Process Biochem. 2012;47(12):1799–806. doi: 10.1016/j.procbio.2012.06.006.
[42] Avelino F, Marques F, Soares AKL, Silva KT, Leitão RC, Mazzetto SE, et al. Microwave-assisted organosolv delignification: A potential eco-designed process for scalable valorization of agroindustrial

wastes. Ind Eng Chem Res. 2019;58:10698–706. doi: 10.1021/acs.iecr.9b01168.
[43] Valevakhin GN, Kontar AA, Galeev ER, Dokhov AI. Intensification of the process of dehydrating alcohol by microwave electromagnetic energy. Proceedings of the International Conference on Antenna Theory and Techniques (ICATT). Kharkiv, Ukraine: 2015. p. 1–2.
[44] de la Hoz A, Díaz-Ortiz A, Moreno A. Review on non-thermal effects of microwave irradiation in organic synthesis. J Microw Power Electromagn Energy. 2007;41(1):44–64. doi: 10.1080/08327823.2006.11688549.
[45] Li H, Zhao Z, Xiouras C, Stefanidis GD, Li X, Gao X. Fundamentals and applications of microwave heating to chemicals separation processes. Renew Sustainable Energy Rev. 2019;114(August):109316. doi: 10.1016/j.rser.2019.109316.
[46] Kuittinen S, Rodriguez YP, Yang M, Keinänen M, Pastinen O, Siika-aho M. Effect of microwave-assisted pretreatment conditions on hemicellulose conversion and enzymatic hydrolysis of norway spruce. Bioenergy Res. 2016;9(1):344–54. doi: 10.1007/s12155-015-9696-9.
[47] Archana BA, Dinesh RD, Paraag RS, Prabhakar SY. Microwave assisted synthesis and pharmacological evaluation of few derivatives of 1, 4-dihydropyridines containing 1, 3, 4-oxadiazoles. Int J Pharm Chem. 2014;4:2–7. doi: 10.7439/ijpc.
[48] Chadni M, Bals O, Ziegler-Devin I, Brosse N, Grimi N. Microwave-assisted extraction of high-molecular-weight hemicelluloses from spruce wood. Comptes Rendus Chim. 2019;22(8):574–84. doi: 10.1016/j.crci.2019.07.002.
[49] See TY, Yusoff R, Chan CH, Ngoh GC. A solid-state microwave method to disrupt biomass microstructure for natural product extraction. Food Bioprod Process. 2018;109:98–106. doi: 10.1016/j.fbp.2018.03.002.
[50] Li MF, Sun SN, Xu F, Sun RC. Microwave-assisted organic acid extraction of lignin from bamboo: Structure and antioxidant activity investigation. Food Chem. 2012;134(3):1392–8. doi: 10.1016/j.foodchem.2012.03.037.
[51] Xue J, Wu T, Dai Y, Xia Y. Electrospinning and Electrospun nanofibers: methods, materials, and applications. Chem Rev. 2019;119(8):5298–415. doi: 10.1021/acs.chemrev.8b00593. Electrospinning.
[52] Dallmeyer I, Ko F, Kadla JF. Electrospinning of technical lignins for the production of fibrous networks. J Wood Chem Technol. 2010;30(4):315–29. doi: 10.1080/02773813.2010.527782.
[53] Huang ZM, Zhang YZ, Kotaki M, Ramakrishna S. A review on polymer nanofibers by electrospinning and their applications in nanocomposites. Compos Sci Technol. 2003;63(15):2223–53. doi: 10.1016/S0266-3538(03)00178-7.
[54] Schreiber M, Vivekanandhan S, Mohanty AK, Misra M. A study on the electrospinning behaviour and nanofibre morphology of anionically charged lignin. Adv Mater Lett. 2012;3(6):476–80. doi: 10.5185/amlett.2012.icnano.336.
[55] Ramakrishna S, Fujihara K, Teo W-E. Electrospinning process. In: Ramakrishna S, Fujihara K, Teo W-E, Lim TC, Ma Z, editors. An introduction to electrospinning and nanofibers. New Jersey: World Scientific Publishing; 2005. p. 90–154.
[56] Long YZ, Yan X, Wang XX, Zhang J, Yu M. Electrospinning: the setup and procedure. In: Ding B, Wang X, Yu J, editors, Electrospinning: Nanofabrication and Applications. Amsterdam: Elsevier; 2018. p. 21–52.
[57] Yuan H, Zhou Q, Zhang Y. Improving fiber alignment during electrospinning. In: Afshari M, editor. Electrospun nanofibers. Amsterdam: Elsevier; 2017. p. 125–47.
[58] Nitti P, Gallo N, Natta L, Scalera F, Palazzo B, Sannino A. Influence of nanofiber orientation on morphological and mechanical properties of electrospun chitosan mats. J Healthc Eng. 2018;2018:3651480. doi: 10.1155/2018/3651480.
[59] García-Mateos FJ, Ruiz-Rosas R, Rosas JM, Rodríguez-Mirasol J, Cordero T. Controlling the composition, morphology, porosity, and surface chemistry of lignin-based electrospun carbon materials. Front Mater. 2019;6(May):1–16. doi: 10.3389/fmats.2019.00114.
[60] Alghoraibi I, Alomari S. Different methods for nanofiber design and fabrication. In: Barhoum A, Bechelany M, Salam A, Makhlouf H, editors. Handbook of Nanofibers. Cham: Springer; 2020. p. 1–32.
[61] Chan CH, Yeoh HK, Yusoff R, Ngoh GC. A first-principles model for plant cell rupture in microwave-assisted extraction of bioactive compounds. J Food Eng. 2016;188:98–107. doi: 10.1016/j.jfoodeng.2016.05.017.
[62] Pan XJ, Sano Y. Atmospheric acetic acid pulping of rice straw IV: Physico-chemical characterization of acetic acid lignins from rice straw and woods. Part 1. Physical characteristics. Holzforschung. 1999;53(5):511–8. doi: 10.1515/HF.1999.084.
[63] Christodoulou X, Velasquez-Orta SB. Microbial electrosynthesis and anaerobic fermentation: an economic evaluation for acetic acid production from CO2 and CO. Environ Sci Technol. 2016;50(20):11234–42. doi: 10.1021/acs.est.6b02101.
[64] Li W, Peng J, Zhang L, Yang K, Xia H, Zhang S, et al. Preparation of activated carbon from coconut shell chars in pilot-scale microwave heating equipment at 60 kW. Waste Manag. 2009;29(2):756–60. doi: 10.1016/j.wasman.2008.03.004.
[65] Xiao W, Han L, Zhao Y. Comparative study of conventional and microwave-assisted liquefaction of corn stover in ethylene glycol. Ind Crops Prod. 2011;34(3):1602–6. doi: 10.1016/j.indcrop.2011.05.024.
[66] Palma V, Barba D, Cortese M, Martino M, Renda S, Meloni E. Microwaves and heterogeneous catalysis: A review on selected catalytic processes. Catalysts. 2020;10(2):246. doi: 10.3390/catal10020246.
[67] Kure N, Hamidon MN, Azhari S, Azhari S, Mamat NS, Yusoff HM, et al. Simple Microwave-assisted synthesis of carbon nanotubes using polyethylene as carbon precursor. J Nanomater. 2017;2017:2474267. doi: 10.1155/2017/2474267.
[68] Islam MA, Hasanuzzaman M, Rahim NA, Nahar A, Hosenuzzaman M. Global renewable energy-based electricity generation and smart grid system for energy security. Sci World J. 2014;2014:197136. doi: 10.1155/2014/197136.
[69] Song LH. Fast, easy preparation of biodiesel using microwave heating. Energy & Fuels. 2006;20(5):2281–3. doi: 10.4028/www.scientific.net/AMR.634-638.764.
[70] Sharifvaghefi S, Zheng Y. Microwave vs conventional heating in hydrogen production via catalytic dry reforming of methane. Resour Chem Mater. 2022;1(3–4):290–307. doi: 10.1016/j.recm.2022.08.003.
[71] Goyal H, Mehdad A, Lobo RF, Stefanidis GD, Vlachos DG. Scaleup of a single-mode microwave reactor. Ind Eng Chem Res. 2020;59(6):2516–23. doi: 10.1021/acs.iecr.9b04491.
[72] Wang SX, Yang L, Stubbs LP, Li X, He C. Lignin-derived fused electrospun carbon fibrous mats as high performance anode materials for lithium ion batteries. ACS Appl Mater Interfaces. 2013;5(23):12275–82. doi: 10.1021/am4043867.

[73] Gellerstedt G, Gustafsson K, Northey RA. Structural changes in lignin during kraft cooking. Nord Pulp Pap Res J. 1988;3(2):87–94. doi: 10.3183/npprj-1988-03-02-p087-094.
[74] Huang D, Li R, Xu P, Li T, Deng R, Chen S, et al. The cornerstone of realizing lignin value-addition: Exploiting the native structure and properties of lignin by extraction methods. Chem Eng J. 2020;402(July):126237. doi: 10.1016/j.cej.2020.126237.
[75] Zhang L, Larsson A, Moldin A, Edlund U. Comparison of lignin distribution, structure, and morphology in wheat straw and wood. Ind Crops Prod. 2022;187(PB):115432. doi: 10.1016/j.indcrop.2022.115432.
[76] Park CW, Youe WJ, Han SY, Kim YS, Lee SH. Characteristics of carbon nanofibers produced from lignin/polyacrylonitrile (PAN)/kraft lignin-g-PAN copolymer blends electrospun nanofibers. Holzforschung. 2017;71(9):743–50. doi: 10.1515/hf-2017-0024.
[77] Kubo S, Kadla JF. Kraft lignin/poly(ethylene oxide) blends: Effect of lignin structure on miscibility and hydrogen bonding. J Appl Polym Sci. 2005;98(3):1437–44. doi: 10.1002/app.22245.
[78] Hu S, Hsieh Y. Ultra fine microporous and mesoporous activated carbon fibers from alkali lignin. J Mater Chem A. 2013;1:11279–88. doi: 10.1039/c3ta12538f.
[79] Shenoy SL, Bates WD, Frisch HL, Wnek GE. Role of chain entanglements on fiber formation during electrospinning of polymer solutions: Good solvent, non-specific polymer-polymer interaction limit. Polymer (Guildf). 2005;46(10):3372–84. doi: 10.1016/j.polymer.2005.03.011.
[80] Mousavioun P. Properties of Lignin and Poly(hydroxybutyrate) Blends [dissertation]. Queensland: University of Technology; 2011.
[81] Gordobil O, Egüés I, Llano-Ponte R, Labidi J. Physicochemical properties of PLA lignin blends. Polym Degrad Stab. 2014;108:330–8. doi: 10.1016/j.polymdegradstab.2014.01.002.
[82] Vincent S, Prado R, Kuzmina O, Potter K, Bhardwaj J, Wanasekara ND, et al. Regenerated cellulose and willow lignin blends as potential renewable precursors for carbon fibers. ACS Sustain Chem Eng. 2018;6(5):5903–10. doi: 10.1021/acssuschemeng.7b03200.
[83] De Vrieze S, Van Camp T, Nelvig A, Hagstrom B, Westbroek P, De Clerck K. The effect of temperature and humidity on electrospinning. J Mater Sci. 2009;44(5):1357–62. doi: 10.1007/s10853-008-3010-6.
[84] Haider A, Haider S, Kang IK. A comprehensive review summarizing the effect of electrospinning parameters and potential applications of nanofibers in biomedical and biotechnology. Arab J Chem. 2018;11(8):1165–88. doi: 10.1016/j.arabjc.2015.11.015.
[85] Villaverde JJ, Li J, Ek M, Ligero P, de Vega A. Native lignin structure of Miscanthus x giganteus and its changes during acetic and formic acid fractionation. J Agric Food Chem. 2009;57(14):6262–70. doi: 10.1021/jf900483t.
[86] Derkacheva O, Sukhov D. Investigation of lignins by FTIR spectroscopy. Macromol Symp. 2008;265(1):61–8. doi: 10.1002/masy.200850507.
[87] Casas A, Oliet M, Alonso MV, Rodríguez F. Dissolution of Pinus radiata and Eucalyptus globulus woods in ionic liquids under microwave radiation: Lignin regeneration and characterization. Sep Purif Technol. 2012;97:115–22. doi: 10.1016/j.seppur.2011.12.032.
[88] Klein SE, Rumpf J, Kusch P, Albach R, Rehahn M, Witzleben S, et al. Unmodified kraft lignin isolated at room temperature from aqueous solution for preparation of highly flexible transparent polyurethane coatings. RSC Adv. 2018;8:40765–77. doi: 10.1039/C8RA08579J.
[89] Sun JX, Sun XF, Zhao H, Sun RC. Isolation and characterization of cellulose from sugarcane bagasse. Polym Degrad Stab. 2004;84:331–9. doi: 10.1016/j.polymdegradstab.2004.02.008.
[90] Moretti De Souza MM, Alonso Bocchini-Martins D, da Costa Carreira Nunes C, Villena MA, Perrone OM, Da Silva R. Pretreatment of sugarcane bagasse with microwaves irradiation and its effects on the structure and on enzymatic hydrolysis. Appl Energy. 2014;122:189–95. doi: 10.1016/j.apenergy.2014.02.020.
[91] Cheng J, Hu SC, Geng ZC, Zhu MQ. Effect of structural changes of lignin during the microwave-assisted alkaline/ethanol pretreatment on cotton stalk for an effective enzymatic hydrolysis. Energy. 2022;254:124402. doi: 10.1016/j.energy.2022.124402.
[92] Rahman OU, Shi S, Ding J, Wang D, Ahmad S, Yu H. Lignin nanoparticles: Synthesis, characterization and corrosion protection performance. New J Chem. 2018;42(5):3415–25. doi: 10.1039/c7nj04103a.
[93] Lundquist K. NMR studies of lignins. 5. Investigation of non-derivatized spruce and birch lignin by 1-H NMR spectroscopy. Acta Chem Scand B. 1981;35:497–501.
[94] Li S, Lundquist K. A new method for the analysis of phenolic groups in lignins by ′H NMR spectrometry. Nord Pulp Pap Res J. 1994;9(3):191–5. doi: 10.3183/npprj-1994-09-03-p191-195.
[95] Fulmer GR, Miller AJM, Sherden NH, Gottlieb HE, Nudelman A, Stoltz BM. NMR chemical shifts of common laboratory solvents as trace impurities NMR chemical shifts of trace impurities: common laboratory solvents, organics, and gases in deuterated solvents relevant to the organometallic chemist. Organometallics. 2017;29(November):2176–9. doi: 10.1021/jo971176v.
[96] Roy R, Jadhav B, Rahman MS, Raynie DE. Characterization of residue from catalytic hydrothermal depolymerization of lignin. Curr Res Green Sustain Chem. 2021;4(August 2020):100052. doi: 10.1016/j.crgsc.2020.100052.
[97] Lawoko BM, Henriksson G, Gellerstedt G. New method for quantitative preparation of lignin-carbohydrate complex from unbleached softwood kraft pulp: lignin-polysaccharide networks I. Holzforschung. 2003;57:69–74. doi: 10.1515/HF.2003.011.
[98] Avelino F, da Silva KT, de Souza Filho MM, Mazzetto SE, Lomonaco D. Microwave-assisted organosolv extraction of coconut shell lignin by Brønsted and Lewis acids catalysts. J Clean Prod. 2018;189:785–96. doi: 10.1016/j.jclepro.2018.04.126.
[99] Yunus R, Salleh SF, Abdullah N, Biak DRA. Effect of ultrasonic pretreatment on low temperature acid hydrolysis of oil palm empty fruit bunch. Bioresour Technol. 2010;101(24):9792–6. doi: 10.1016/j.biortech.2010.07.074.
[100] Sun RC, Tomkinson J. Comparative study of lignins isolated by alkali and ultrasound-assisted alkali extractions from wheat straw. Ultrason Sonochem. 2002;9(2):85–93. doi: 10.1016/S1350-4177(01)00106-7.
[101] Toledano A, García A, Mondragon I, Labidi J. Lignin separation and fractionation by ultrafiltration. Sep Purif Technol. 2010;71(1):38–43. doi: 10.1016/j.seppur.2009.10.024.
[102] García A, Alriols MG, Llano-Ponte R, Labidi J. Ultrasound-assisted fractionation of the lignocellulosic material. Bioresour Technol. 2011;102(10):6326–30. doi: 10.1016/j.biortech.2011.02.045.
[103] Mothé CG, De Miranda IC. Characterization of sugarcane and coconut fibers by thermal analysis and FTIR. J Therm Anal Calorim. 2009;97(2):661–5. doi: 10.1007/s10973-009-0346-3.

[104] Tejado A, Peña C, Labidi J, Echeverria JM, Mondragon I. Physicochemical characterization of lignins from different sources for use in phenol-formaldehyde resin synthesis. Bioresour Technol. 2007;98(8):1655–63. doi: 10.1016/j.biortech.2006.05.042.

[105] Pang B, Yang S, Fang W, Yuan TQ, Argyropoulos DS, Sun RC. Structure-property relationships for technical lignins for the production of lignin-phenol-formaldehyde resins. Ind Crops Prod. 2017;108(March):316–26. doi: 10.1016/j.indcrop.2017.07.009.

[106] Chen G, Andries J, Spliethoff H, Leung DYC. Experimental investigation of biomass waste (rice straw, cotton stalk, and pine sawdust) pyrolysis characteristics. Energy Sources. 2003;25(4):331–7. doi: 10.1080/00908310390142361.

[107] Sun RC, Tomkinson J, Jones LG. Fractional characterization of ash-AQ lignin by successive extraction with organic solvents from oil palm EFB fibre. Polym Degrad Stab. 2000;68:111–9. doi: 10.1016/S0141-3910(99)00174-3.